

RESEARCH ARTICLE

Spatial reasoning with augmented points: Extending cardinal directions with local distances

Reinhard Moratz

School of Computing and Information Science, University of Maine, ME, USA

Jan Oliver Wallgrün

Department of Geography, The Pennsylvania State University, PA, USA

Received: March 17, 2012; returned: June 24, 2012; revised: September 7, 2012; accepted: November 1, 2012.

Abstract: We present an approach for supplying existing qualitative direction calculi with a distance component to support fully fledged positional reasoning. The general underlying idea of augmenting points with local reference properties has already been applied in the \mathcal{OPRA}_m calculus. In this existing calculus, point objects are attached with a local reference direction to obtain oriented points and able to express relative direction using binary relations. We show how this approach can be extended to attach a granular distance concept to direction calculi such as the cardinal direction calculus or adjustable granularity calculi such as \mathcal{OPRA}_m or the Star calculus. We focus on the cardinal direction calculus and extend it to a multi-granular positional calculus called \mathcal{EPR}_m . We provide a formal specification of \mathcal{EPR}_m including a composition table for \mathcal{EPR}_2 automatically determined using real algebraic geometry. We also report on an experimental performance analysis of \mathcal{EPR}_2 in the context of a topological map-learning task proposed for benchmarking qualitative calculi. Our results confirm that our approach of adding a relative distance component to existing calculi improves the performance in realistic tasks when using algebraic closure for consistency checking.

Keywords: qualitative spatial reasoning, direction relations, distance relations, topological robot mapping, cardinal directions, SparQ, granularity, constraint networks

1 Introduction

The way humans as researchers (e.g., physicists) and engineers geometrically model physical space differs fundamentally from human spatial concepts involved in reasoning about everyday situations. In particular, they rely on *quantitative* representations based on measures that assess properties in relation to established units of measurement, which have to be generally available. In contrast, humans in everyday situations perform spatial reasoning to accomplish routine tasks in a timely and efficient manner. A key element in this process is to make a decision between a small set of possible actions. Human thinking is therefore known to leave out unnecessary details to speed up the inference process [12,38]. Condensed representations are employed that only represent relevant features of the environment. Such *qualitative* representations provide mechanisms which characterize essential properties of objects or configurations and only make relatively coarse distinctions between spatial relations and configurations, and typically rely on relative comparisons rather than measuring.

Qualitative spatial and temporal calculi are formally defined and investigated in the research area of qualitative spatial reasoning (QSR) [4, 5, 44]. QSR aims to model human commonsense reasoning about space and time using qualitative relations for different spatial aspects, such as topology (e.g., “included in”), direction (“to the left of”), and position as a combination of direction and distance, holding between elementary spatial entities such as points or regions. Coarse spatial knowledge can be used to represent incomplete and under-determined knowledge in a systematic way. This is especially useful if the task is to describe features of classes of configurations rather than features of individual configurations. As an example, the observation that the goalkeeper usually stands in front of the goal is true for a variety of ball games. A more specific expression about his or her position typically would have to refer to the corresponding configuration of a specific sport. In a similar way, descriptions of allowed or desired spatial behavior are abstractions that map infinite sets of possible quantitative configurations or trajectories to a single qualitative description. For instance consider a sea navigation rule such as “When two power-driven vessels are meeting *head-on* or *nearly head-on* courses so as to involve risk of collision, each shall alter her course to *starboard* so that each shall *pass on the port side* of the other.” (example taken from [8]). Qualitative spatial calculi have been shown to be able to express and formalize the relevant spatial knowledge in such scenarios as well as perform high-level symbolic reasoning with it [27, 39, 53, 55].

The focus in research on QSR and qualitative spatial calculi over the past decades has been on topological reasoning about regions [9, 40, 43] and positional reasoning about point configurations [10, 11, 21, 29, 36, 42]. Qualitative calculi for positional reasoning are concerned with direction and distance relations. A recent trend in this area is the usage of parameterized multi-granular calculi [29, 36, 42] that allow for adapting the directional or distance resolution to make finer distinctions whenever this is required in a particular application. The possibility to use finer qualitative distinctions can be viewed as a stepwise transition to quantitative knowledge. The idea of using context-dependent direction and distance intervals for the representation of spatial knowledge can be traced back to Clementini, di Felice, and Hernandez [3]. However, only limited cases of reasoning were considered in their work. Finer distinctions based on continuous interval borders were suggested in previous work by the authors of this paper [33, 34]. But again only limited cases of rea-

soning were supported by this approach. In contrast, the calculus we will propose in this paper will make direct use of general purpose constraint propagation.

Qualitative spatial calculi for topological aspects (e.g., the 9-intersection approach [9] and RCC-8 [40]) and cardinal direction (e.g., the models in [10, 16, 21, 42]), make use of *binary* relations (“contained-in” or “north-of”) to express spatial knowledge and the defined relation algebraic operations to perform elementary reasoning from relation algebras or non-associative algebras over binary relations [18, 22, 47]. In contrast, aspects such as relative direction or distance [2, 11, 17, 20, 31] are typically more naturally expressed using *ternary* relations, e.g., “object C is to the left of object B as seen from A” or “C is more distant from A than B.” Our aim in this paper is to extend multi-granular directional qualitative reasoning formalisms with a granular distance concept for fully fledged positional reasoning, while staying within the framework of binary qualitative spatial reasoning. The method we propose is a generalization of the approach already taken in the $OPRA_m$ calculus [29, 36], in which point objects are augmented with an internal reference *direction* to obtain oriented points as basic entities. Even if the spatial objects are, from a geometrical point of view, infinitesimally small points, locally available reference measures are attached. The same principle works also with local reference *distances* which we call *elevations*. We refer to the general approach of attaching reference features to points as *hidden feature attachment* and the points with attached hidden features as *augmented points*. We apply the hidden feature attachment approach to design an extended version of the Cardinal Direction Calculus [10, 21] called $\mathcal{E}PRA_m$, supporting positional reasoning based on absolute direction as well as distance information. We also discuss how other directional calculi such as $OPRA_m$ [29, 36] or the Star calculus [42] can be extended using the same approach.

In the second part of the paper, we focus on the investigation of $\mathcal{E}PRA_m$ as a calculus for performing positional reasoning with absolute direction and relative distance information. This part comprises the derivation of a formal specification of $\mathcal{E}PRA$ with its converse and composition operations as well as an experimental analysis using a proposed benchmark application for qualitative calculi, involving the task of deriving the global layout of indoor environments from local observations [50]. We also demonstrate that algebraic closure is not sufficient to decide consistency of atomic networks. Nevertheless, our benchmarking experiments show an improved performance of $\mathcal{E}PRA_2$ over the Cardinal Direction Calculus.

2 Background

QSR aims at capturing human-level concepts of space using finite sets of relations abstracting from quantitative details but preserving the information relevant for spatial decision processes and reasoning [13, 14]. In this section, we recapitulate the most important concepts and definitions of QSR and qualitative spatial calculi; introduce the notations used in the remainder of the text; and provide an overview on related work forming the motivation for our approach.

In the context of this work, a *qualitative spatial calculus* is formally defined as a triple $C = (\mathcal{D}, \mathcal{B}, \mathcal{O})$. The domain \mathcal{D} is the potentially infinite set of spatial objects considered by the calculus, e.g., the sets of all points, lines, or regions in the plane. \mathcal{B} is a set of n -ary relations over \mathcal{D} referred to as *base relations*. For an n -tuple of objects from \mathcal{D} exactly one

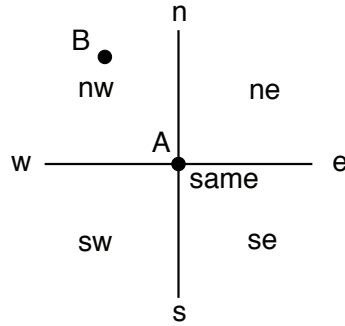


Figure 1: Qualitative spatial directions in the cardinal direction calculus.

relation from \mathcal{B} holds, meaning \mathcal{B} is jointly-exhaustive and pairwise-disjoint (JEPD). \mathcal{O} is a set of operations defined on \mathcal{B} that will be explained further below.

For instance, the Cardinal Direction Calculus (CDC) [10, 21], which will play an important role in this paper, is a calculus over binary relations between points in the plane ($\mathcal{D} = \mathbb{R}^2$). For two points A, B in the 2D plane, the CDC distinguishes the nine qualitative direction relations that are depicted in Figure 1. Point A induces linear sectors $n, w, s,$ and e corresponding to north, west, south, east in the absolute cardinal direction reference system. On the other hand, $ne, se, sw,$ and nw are 2-dimensional quadrants. Each relation corresponds to one of these mutually exclusive areas around point A in which B can be located. For Figure 1, the relation $B \text{ nw } A$ holds (e.g., this corresponds to the natural language expression “ B is north-west of A ”). The case in which point B coincides with point A is denoted by the base relation `same` (also referred to as `equal` or `eq` in the literature).

The set of base relations of a qualitative calculus \mathcal{C} induces another set of relations \mathcal{R} called the *general relations*. It consists of all unions of relations of base relations including the empty relation (union of no base relations) and the universal relation (union of all base relations). We follow the often used notation of writing general relations as sets of the constituent base relations, e.g., $\{n, nw, w\}$. The empty relation is written as \emptyset , while \mathcal{U} is used as an abbreviation for the universal relation. General relations can express incomplete or uncertain information on a qualitative level. For instance, $B\{n, nw\}A$ means that B is either to the north *or* to the northwest of A .

A set of spatial facts using general relations from a given qualitative calculus holding between a set of spatial objects can be depicted as a *qualitative constraint network* (QCN) as shown in Figure 2(a). The nodes in the graph stand for spatial object variables $V = \{O_1, O_2, \dots, O_m\}$ ranging over the domain \mathcal{D} . The arcs, on the other hand, represent the spatial constraints C_{ij} that have to hold between the objects O_i and O_j and are, hence, given in terms of general relations from the calculus at hand. For nodes that are not connected by an arc the implicit constraint is the universal relation \mathcal{U} . A QCN is *consistent* if one can assign values from the domain to all object variables such that all constraints are satisfied. Such an assignment is called a *solution* of the constraint satisfaction problem represented by the QCN. A QCN in which all constraints are base relations of the given calculus is called *atomic* or a *scenario*. A QCN which contains disjunctive constraints can be *refined* into multiple scenarios by removing all except one base relation from the disjunctive constraints

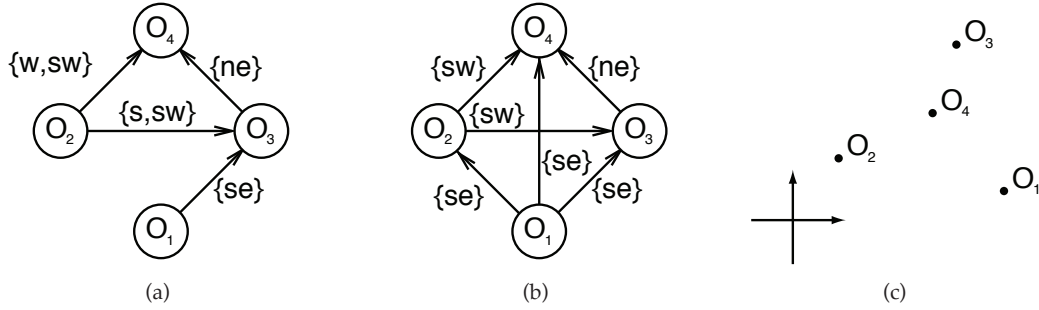


Figure 2: (a) A qualitative constraint network using relations of the cardinal direction calculus as constraints and (b) one of its scenarios which happens to be consistent. (c) shows one possible solution corresponding to this scenario.

(see Figure 2(b)). Each solution corresponds to one particular *consistent* scenario of the original QCN as illustrated in Figure 2(c).

The last component of a qualitative calculus is the set \mathcal{O} of operations defined on the general set of relations \mathcal{R} . In the case of a binary calculus (a calculus over binary relations), it consists of five operations $\mathcal{O} = (\cap, \cup, \bar{}, \sim, \circ)$. \cap , \cup , and $\bar{}$ are the standard set operations of intersection, union, and complement (with respect to \mathcal{D}^2). The *converse* operation \sim is a unary operation that transposes the arguments of the tuples in a relation r and, hence, is formally defined as $r^\sim = \{(A, B) \mid (B, A) \in r\}$. Clearly, in the cardinal direction calculus, the converse of n is s , the converse of nw is se , etc.

The binary *composition* operation \circ allows for inferring the relation between two objects A and C by combining the relation r holding between A and B with the relation s holding between B and C : $r \circ s = \{(A, C) \mid \exists B \in \mathcal{D} : (A, B) \in r \wedge (B, C) \in s\}$. In the cardinal direction calculus, the composition of n and nw is nw and the composition of nw and ne is the universal relation \cup . The composition is the fundamental operation for propagating spatial information and inferring new knowledge in QSR as well as the underlying mechanism in the most common consistency checking approaches. Both, inferring new knowledge and consistency checking are traditionally based on a procedure called *algebraic closure* or *path consistency algorithm* [25, 28, 48] running in $O(n^3)$ time. This algorithm performs the following operation for all triples of variables O_i, O_j, O_k in a QCN to refine the constraint holding between O_i and O_k : $C_{ik} = C_{ik} \cap (C_{ij} \circ C_{jk})$. This is done until a fixpoint is reached or a resulting relational constraint becomes the empty relation which indicates that the input network is inconsistent. For certain calculi, no occurrence of the empty relation means the network is consistent. For most calculi, however, this is only the case if the input network is a scenario and a backtracking search has to be employed to split the constraints and then apply the algebraic closure procedure potentially exploiting previously identified maximal tractable subsets [19, 37, 43].

In a qualitative spatial calculus defined in this way, the intersection, union, and complement operations are always closed over the set of general relations \mathcal{R} . Whether this also holds for the converse and composition operations depends on the definition of the base relations. If this is not the case, these operations need to be redefined as weaker versions

in order to enforce closure with respect to \mathcal{R} . This is achieved by taking the union of the smallest set of base relations that contains the result of the strong operation. The weak converse operation \sim_w is then defined as $r \sim_w = \{B \in \mathcal{B} \mid B \cap (r \sim) \neq \emptyset\}$ and the weak composition operation as $r \circ_w s = \{B \in \mathcal{B} \mid B \cap (r \circ s) \neq \emptyset\}$. Weak operations *may* lead to information loss when applying a sequence of operations and a reduction in the effectiveness of the mentioned standard techniques for checking consistency. While the converse operation is strong in almost all binary spatial calculi, the composition operation, typically defined as a look-up table called a composition table, is often weak. As a result, the algebra formed by the five operations in \mathcal{O} together with \emptyset and \cup becomes a non-associative relation algebra [22, 23, 26] instead of a full relation algebra in the sense of Tarski [18, 47].

In ternary qualitative calculi such as the Singlencross or Doublecross calculus [11] or the Flipflop calculus [20], the intersection, union, and complement operations are defined analogously to the binary case. The converse operation, which has the purpose of generating permutations of object tuples, has to be replaced by multiple operations for generating all possible permutations of a triple. Traditionally, ternary spatial calculi only define a single binary composition operation. However, it has been argued in [7] that the generalization of composition to the ternary case as a binary operation is insufficient and that the correct generalization is a ternary operator taking three relations as input. We do not go any further into the details of ternary calculi here as the focus of this paper is the development of qualitative positional reasoning in a binary relational framework.

3 Adding relative distance to binary point calculi

Fully fledged qualitative positional reasoning requires representational formalisms, i.e., qualitative spatial calculi, that combine direction information—either in absolute or relative form—with distance information. We start our design of suitable calculi with a contemplation of the developments that led to the \mathcal{OPRA}_m calculus: a calculus that supports reasoning about relative direction but does not include distance information.

Figure 3 shows three representatives of spatial calculi able to express relative direction in the chronological order in which they have been invented. Arguably the most natural way to express relative direction is by using ternary relations describing where object C is with respect to object B when seen from A (where A, B, C here are assumed to be points in the plane). This approach has, for instance, been taken in Freksa’s Doublecross calculus [11] shown in Figure 3(a) which distinguishes 15 base relations (assuming that A and B do not coincide). Other examples following this approach are the Flipflop calculus [20] and its refinements [46] and the Singlencross calculus [11].

The Dipole calculus [30, 32] shown in Figure 3(b) proposed approximately 10 years later¹ is able to express the relative direction of extended objects with an intrinsic direction represented by oriented straight line segments called dipoles. Details about the distinguished dipole relations can be found in [32]. In the context of this work, the important point is that the Dipole calculus is a *binary* calculus. However, it can only be applied when the objects involved can be adequately represented by dipoles. In many potential application scenarios, the objects do not have a meaningful length feature and are best represented as points.

¹Although earlier versions existed before that time [45].

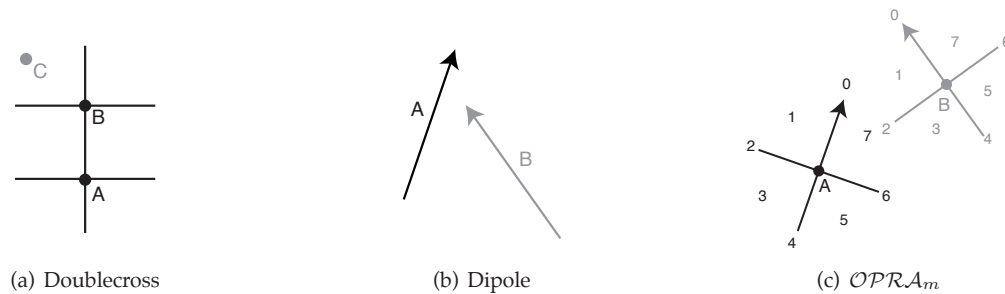


Figure 3: Examples of direction calculi.

The $OPRA_m$ calculus [29,36] (see Figure 3(c)) addresses this issue by attaching intrinsic orientations to point objects leading to the concept of *oriented points*. It is also an example of a multi-granular calculus in which a granularity parameter m can be used to instantiate relational schemes with different resolutions. Given the granularity parameter m , a partitioning of the plane into $4m$ direction sectors is established for each of the two oriented points A and B involved in a relation. The respective relations are written as $A \mathbin{\angle}_m^b B$ where a is the direction sector of A that contains B and b is the direction sector of B that contains A (cf. again Figure 3(c)). Oriented points can be seen as dipoles with an infinitely small length. In this conceptualization, the length of the objects involved no longer has any importance and objects without an intrinsic orientation can be provided with one, for instance pointing towards a particular other object.

Essentially, this method attaches a feature which is used as a local reference to an object in the 2D-plane which is geometrically still a featureless point. We call this principle *hidden feature attachment* and the extended point objects *augmented points*. This approach can be adapted to other modalities than direction. In the following, we employ it to introduce the concept of *elevated points* able to represent distance information. We then develop new spatial calculi by extending existing approaches, in particular the CDC, with a distance concept.

3.1 Elevated point and basic distance relations

In analogy to the attachment of a reference direction to a featureless point, we can extend point-based binary direction calculi with a local reference distance and then express relative distance relations by comparing these reference distances. We refer to these reference distances as *elevations* due to an analogy with local basic perceptions of a cognitive agent forming the basis for establishing distance categories: we imagine that the point standing for a particular location is *elevated* above the 2D-plane (see point A in Figure 4) representing, for instance, the viewpoint of a human observer who visually perceives the environment. From this observer perspective, Gibson's insights about natural perspective [15] motivate the availability of depth clues which let the observer distinguish local distances based on a comparison of their distance with this elevation or height value. Although this analogy makes use of three-dimensional space, our model refers to the 2D plane.

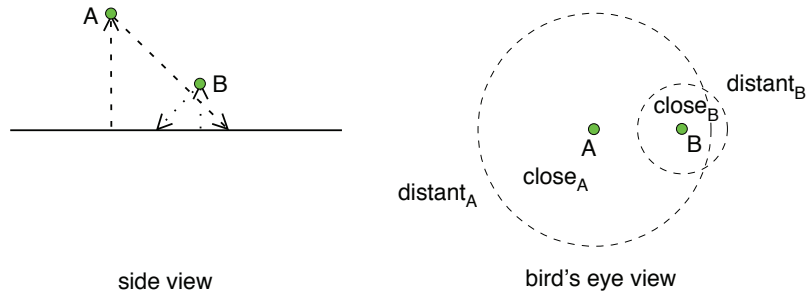


Figure 4: Qualitative spatial distance relations between two points based on the notion of elevation.

We can interpret the elevation as describing a circle around the point providing a reference distance, when projected to the ground plane. As an abstraction, every salient location/point (e.g., the second point B in Figure 4) can be assigned such a reference distance. This elevation can also be unspecified or unknown leading to disjunctions in the distance relations defined in the following. We refer to such points with an attached elevation feature as *elevated points*, or simply *e-points*.

Distances between two e-points A and B can now be locally compared using the projections of their elevations onto the 2D plane and considering the resulting partitioning of the ground plane into three partitions called *close*, *equal*, and *distant* for each of the two points (Figure 4). Considering in which of the three partitions the other point is located, allows us to distinguish nine binary distance relations for points with different locations. Similar to the notation of $OPRA_m$ relations, we write the two distance components on top of each other where the top one is the distance of A with respect to B , while the bottom one is the distance of B with respect to A :

distant , equal , close , distant , equal , close , distant , equal , close
distant , distant , distant , equal , equal , equal , close , close , close

The relation depicted in Figure 4 has the following expression:

$$A \begin{array}{c} \text{distant} \\ \text{close} \end{array} B$$

To formally specify the e-point relations, we use two-dimensional continuous space, in particular \mathbb{R}^2 . Every e-point S on the plane is an ordered pair of a point \mathbf{p}_S represented by its Cartesian coordinates x_S and y_S , with $x_S, y_S \in \mathbb{R}$, and an internal reference distance $\delta_S \in \mathbb{R}^+$ which corresponds to the elevation height in the cognitive motivation.

$$S = (\mathbf{p}_S, \delta_S), \quad \mathbf{p}_S = (x_S, y_S)$$

The metrical distance between e-points A and B is their Euclidean distance:

$$|A - B| = \sqrt{(x_A - x_B)^2 + (y_A - y_B)^2}$$

Then the nine distance relations in configurations with $\mathbf{p}_A \neq \mathbf{p}_B$ are defined in the following way:

$$\begin{aligned}
 \delta_A < |A - B| > \delta_B &\iff A \begin{array}{l} \text{distant} \\ \text{distant} \end{array} B \\
 \delta_A < |A - B| = \delta_B &\iff A \begin{array}{l} \text{equal} \\ \text{distant} \end{array} B \\
 \delta_A < |A - B| < \delta_B &\iff A \begin{array}{l} \text{close} \\ \text{distant} \end{array} B \\
 \delta_A = |A - B| > \delta_B &\iff A \begin{array}{l} \text{distant} \\ \text{equal} \end{array} B \\
 \delta_A = |A - B| = \delta_B &\iff A \begin{array}{l} \text{equal} \\ \text{equal} \end{array} B \\
 \delta_A = |A - B| < \delta_B &\iff A \begin{array}{l} \text{close} \\ \text{equal} \end{array} B \\
 \delta_A > |A - B| > \delta_B &\iff A \begin{array}{l} \text{distant} \\ \text{close} \end{array} B \\
 \delta_A > |A - B| = \delta_B &\iff A \begin{array}{l} \text{equal} \\ \text{close} \end{array} B \\
 \delta_A > |A - B| < \delta_B &\iff A \begin{array}{l} \text{close} \\ \text{close} \end{array} B
 \end{aligned}$$

In configurations in which the two points have the same position (i.e., $\mathbf{p}_A = \mathbf{p}_B$), called **same cases**, their reference distances are compared in the following way:

$$\begin{aligned}
 |A - B| = 0 \wedge \delta_A > \delta_B &\iff A \begin{array}{l} \text{close} \\ \text{same} \end{array} B \\
 |A - B| = 0 \wedge \delta_A = \delta_B &\iff A \begin{array}{l} \text{equal} \\ \text{same} \end{array} B \\
 |A - B| = 0 \wedge \delta_A < \delta_B &\iff A \begin{array}{l} \text{distant} \\ \text{same} \end{array} B
 \end{aligned}$$

Altogether, these 12 distance relations can be seen as the base relations of a coarse distance calculus. We now introduce a granularity parameter m to allow for the distance modality to have an adjustable granularity (for the concept of scalable granularity compare [36]). We define the basic schema from Figure 4 with three partitions to correspond to $m = 2$. In addition, we modify the notation scheme for the relations of this purely distance-based calculus to be $A \circlearrowleft_i^j B$ and allowing numbers 1, 2, 3 to be used in the relation names instead of the mnemonic names *close*, *equal*, and *distant* (e.g., $A \circlearrowleft_{\frac{1}{2}} B$ instead of $A \circlearrowleft_{\text{equal}}^{\text{close}} B$). Figure 5 shows the corresponding schema for granularity $m = 4$. The intuition behind this schema is the empirical observation that subjective distances can be modeled as functions of objective distances with the property that larger distances are represented in a coarser resolution [1]. Another design criterion was the intended property that base relations should have single base relations as converses (strong converse operation). As a result, distances smaller than *equal* have equidistant dividing borders and the distances greater than *equal* are multiplicative inverses to guarantee single base relations as converses in the case of **same** relations. The granularity parameter m corresponds to the number of dividing borders including the **same** case.

To define the schema for qualitative relative distances $A \circlearrowleft_i^j B$ ($0 < i, j < 2m$) between e-point pairs with $\mathbf{p}_A \neq \mathbf{p}_B$ formally, we first define the boundaries of the distance partitioning around A to be given by a function $b_A(i)$ with $0 \leq i \leq 2m$ and i being an even numbers (written as $i \equiv_2 0$ for $i \bmod 2 = 0$):

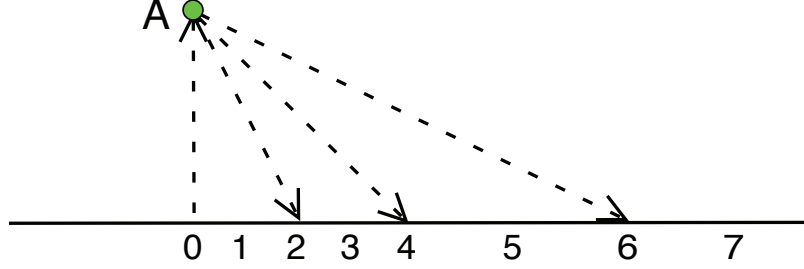


Figure 5: Qualitative spatial distances for granularity parameter $m = 4$: four projections corresponding to $\delta * 0$, $\delta * 1/2$, δ , and $\delta * 2$ are used to divide the plane into eight ($= 2m$) partitions numbered from 0 to 7.

$$b_A(i) = \begin{cases} \infty & \text{if } i = 2m \\ \frac{i \delta_A}{m} & \text{if } i \leq m \\ \frac{m \delta_A}{2m-i} & \text{otherwise} \end{cases} \quad (1)$$

The distance component i in $A \circ_m^j B$, with $0 < i < 2m$, is then defined as

$$A \circ_m^* B \iff (i \equiv_2 0 \wedge |A - B| = b_A(i)) \vee (i \equiv_2 1 \wedge b_A(i-1) < |A - B| < b_A(i+1)) \quad (2)$$

where the $*$ stands for an arbitrary value for j . And analogously for the distance partition around B and parameter j in $A \circ_m^j B$:

$$b_B(j) = \begin{cases} \infty & \text{if } j = 2m \\ \frac{j \delta_B}{m} & \text{if } j \leq m \\ \frac{m \delta_B}{2m-j} & \text{otherwise} \end{cases} \quad (3)$$

$$A \circ_m^j B \iff (j \equiv_2 0 \wedge |A - B| = b_B(j)) \vee (j \equiv_2 1 \wedge b_B(j-1) < |A - B| < b_B(j+1)) \quad (4)$$

For the same relations in which the two points have the same position (i.e., $\mathbf{p}_A = \mathbf{p}_B$), the formal schema $A \circ_m^i{}_{same} B$ ($0 < i < 2m$) for general granularity parameter m is given by:

$$\begin{aligned}
 A \circ_{same}^i B &\iff (i \equiv_2 0 \wedge \delta_B = b_A(i)) \\
 &\quad \vee \\
 &\quad (i \equiv_2 1 \wedge b_A(i-1) < \delta_B < b_A(i+1))
 \end{aligned} \tag{5}$$

where $b_A(i)$ is the boundary function already defined above.

3.2 $\mathcal{EPR}\mathcal{A}_m$: Combining the distance relations with CDC

We now combine the idea of hidden feature attachment to represent distance information, which led to the concept of elevated points, with the CDC calculus for cardinal directions introduced in Section 2. The partitioning of the CDC as shown in Figure 1 can be seen as the coarsest level in a multi-granular calculus using the same partitioning approach employed in $\mathcal{OPR}\mathcal{A}_m$ (cf. Figure 3(c)) but with the 0 direction always pointing *up* or *north*. We call this multi-granular version \mathcal{CDC}_m and define the coarsest level to correspond to $m = 2$. For $m = 4$, two more partitioning lines would be introduced using 45° angles to generate a partition into 16 direction sectors (8 linear and 8 two-dimensional) numbered from 0 to 15 in counterclockwise order. We restrict ourselves to even number for the granularity parameter m . Each instance of \mathcal{CDC}_m for a given m could in principle also be defined as a version of the Star calculus [42], which is more general as it allows for non-equally sized sectors in the partition.

The distance and direction components can in principle be combined using different granularity parameters for each. In this paper, however, we follow the approach of coupling the two granularities by using a single granularity parameter m for both. As the domain of e-points used to define distance relations subsumes the domain of points in the plane of CDC, the combined calculus $\mathcal{EPR}\mathcal{A}_m$ ² also has e-points as its domain. Figure 6 illustrates the resulting partitioning scheme of $\mathcal{EPR}\mathcal{A}_m$ using fully drawn circles to show the respective elevations and dashed circles for the remaining boundaries of the distance partitions (only appearing for $m = 4$).

We write $\mathcal{EPR}\mathcal{A}_m$ relations in which the two involved points do not coincide using the following notation: $A \circ_{d_1}^m \circ_{d_2}^a B$ where m is the granularity parameter, a is the number of the cardinal direction sector of B that contains A , d_1 is the number of the distance partition of A which contains B , and d_2 is the distance partition of B which contains A . Relations in which A and B coincide (called *same* relations again) are written as \circ_{same}^d with d being the distance partition of A which contains *the elevation circle of B* . In the case of $m = 2$, we also use *close*, *equal*, *distant* and *n*, *nw*, *w*, etc. instead of the partition numbers. Figure 6(a), for instance, shows the $\mathcal{EPR}\mathcal{A}_2$ relation $\circ_1^2 \circ_1^7$ or, alternatively, $\circ_{close}^{distant}$, while Figure 6(b) shows the *same* relation \circ_{same}^1 (or \circ_{same}^{close}). In Figure 6(c), we see an example for $m = 4$, namely the $\mathcal{EPR}\mathcal{A}_4$ relation $\circ_3^4 \circ_5^{13}$.

We will give a complete formal definition of $\mathcal{EPR}\mathcal{A}$ in Section 4 including a specification of the important converse and composition operations.

²The first two letters of the symbol $\mathcal{EPR}\mathcal{A}_m$ stand for elevated point.

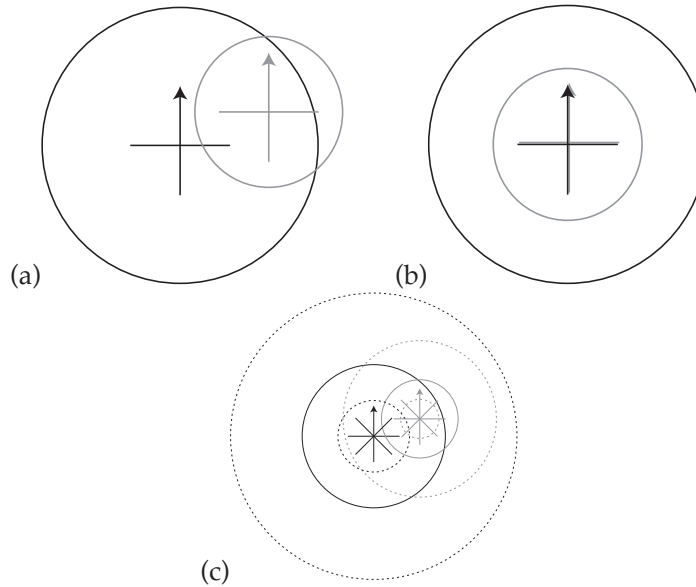


Figure 6: (a) $\mathcal{EPR}\mathcal{A}_2$ relation ${}_2\textcircled{*} ne \overset{distant}{close}$, (b) $\mathcal{EPR}\mathcal{A}_2$ relation ${}_2\textcircled{*} \overset{close}{same}$, and (c) $\mathcal{EPR}\mathcal{A}_4$ relation ${}_4\textcircled{*} 13 \overset{5}{3}$.

3.3 Extending other directional calculi

The same approach of defining distance relations by attaching a reference distance to spatial entities can naturally be employed to other calculi, for instance other directional calculi such as the absolute Star calculus and the relative $\mathcal{OPR}\mathcal{A}_m$ calculus. The Star calculus can be seen as a more general version of the CDC calculus in which the planar sectors do not all have to be of the same size. The domain of the extended version would again consist of elevated points as in $\mathcal{EPR}\mathcal{A}_m$ and the extension would be analogous to that described for CDC.

$\mathcal{OPR}\mathcal{A}_m$ deals with the relative direction of oriented points (points with an intrinsic reference direction) in the plane. Hence, one would need to combine the concepts of oriented point and elevated point to define points with an intrinsic orientation and elevation as the domain for the combined calculus. Formally the domain is $\mathbb{R}^2 \times [0..360) \times \mathbb{R}^+$ (the set of oriented and elevated points) and the resulting eo-points can be written as triples $((x_A, y_A), \theta_A, \delta_A)$ with the first component being Cartesian coordinates x_A and y_A of the point, θ_A giving the orientation, and δ_A the elevation. Figure 3 illustrates the resulting distance and direction partitions using again a single granularity parameter. Relations of the extended calculus, which we refer to as $\mathcal{EOPR}\mathcal{A}_m$ ³, are written in the following way: when the two involved points do not coincide, the relations are written as ${}_m\angle_{a_1}^{a_2} \overset{a_2}{d_1}$ with m , d_1 , and d_2 being the same as for $\mathcal{EPR}\mathcal{A}$, while a_1 and a_2 correspond to the direction components of the original $\mathcal{OPR}\mathcal{A}_m$ calculus (cf. again Figure 3). Relations for coinciding points (same cases) are analogously written as ${}_2\angle_{same}^{a d}$. The relations shown in Figure 7

³The first three letters of the symbol $\mathcal{EOPR}\mathcal{A}_m$ stand for elevated oriented point.

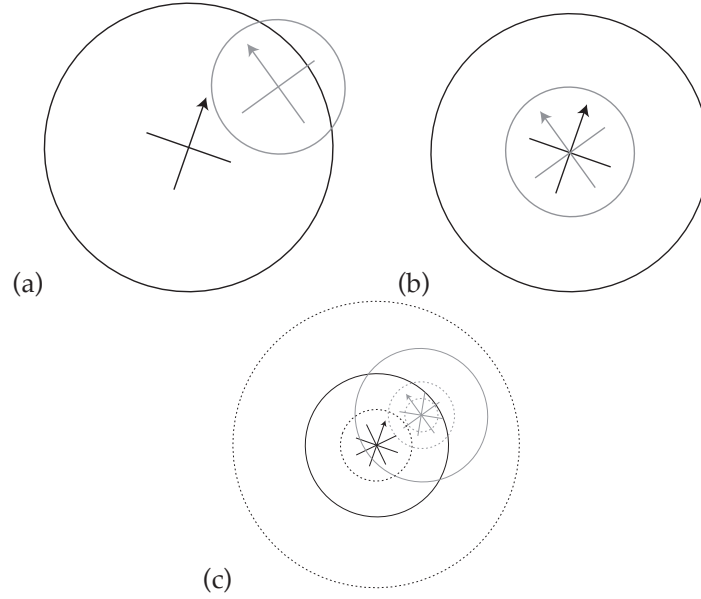


Figure 7: (a) \mathcal{EOPRA}_2 relation ${}_2\angle_7^1 \text{distant}$, (b) \mathcal{EOPRA}_2 relation ${}_2\angle_{\text{same}}^1 \text{close}$, and (c) \mathcal{EOPRA}_4 relation ${}_4\angle_{15}^3 \text{ } \frac{5}{3}$.

correspond to those from Figure 6: (a) shows the relation ${}_2\angle_7^1 \text{distant}$, (b) shows ${}_2\angle_{\text{same}}^1 \text{close}$, and (c) shows ${}_4\angle_{15}^3 \text{ } \frac{5}{3}$.

4 Specification and analysis of \mathcal{EPRA}

In the following, we give a formal specification of the \mathcal{EPRA} calculus and report on how we were able to automatically derive a composition table. Our specification follows the formal definition of a qualitative spatial calculus given in Section 2 as a triple $\mathcal{EPRA} = (\mathcal{D}_{\mathcal{EPRA}}, \mathcal{B}_{\mathcal{EPRA}}, \mathcal{O}_{\mathcal{EPRA}})$. From the operations in $\mathcal{O}_{\mathcal{EPRA}}$, only the converse and composition operations need to be defined in a calculus specific way. Intersection, union, and complement keep their set-theoretic meaning. While we will define the base relations and converse operation for arbitrary granularity parameter m , the definition of the composition operation is restricted to granularity $m = 2$. The reason is that in contrast to the other components, determining the composition table is a challenging problem and no simple closed formula exists as is the case for the converse. We also investigate the question whether algebraic closure is sufficient to decide the consistency of atomic \mathcal{EPRA} networks and provide a counterexample that shows that this is not the case.

4.1 Domain and base relations

As already described in Section 3, the domain $\mathcal{D}_{\mathcal{EPRA}}$ of \mathcal{EPRA}_m is the set of elevated points: $\mathcal{D}_{\mathcal{EPRA}} = \mathbb{R}^2 \times \mathbb{R}^+$. The set of base relations $\mathcal{B}_{\mathcal{EPRA}}$ for \mathcal{EPRA}_m consists of the set of *same* relations $\mathcal{B}_{\mathcal{EPRA}, \text{same}}$ and the set $\mathcal{B}_{\mathcal{EPRA}, \text{distinct}}$ of relations in which the two

related e-points do not coincide ($\mathcal{B}_{\mathcal{EPR}\mathcal{A}} = \mathcal{B}_{\mathcal{EPR}\mathcal{A},\text{same}} \cup \mathcal{B}_{\mathcal{EPR}\mathcal{A},\text{distinct}}$). The set of **same** relations consists of relations written in the form ${}_m \circledast_{\text{same}}^d$. More precisely:

$$\mathcal{B}_{\mathcal{EPR}\mathcal{A},\text{same}} = \{ {}_m \circledast_{\text{same}}^i \mid 0 < i < 2m \}$$

where i is the number of the distance sector as defined in Eq. 5 (or, alternatively, the abbreviated sector names introduced for $m = 2$ in Section 3).

The other set of base relations $\mathcal{B}_{\mathcal{EPR}\mathcal{A},\text{distinct}}$ consists of relations written as ${}_m \circledast a_i^j$:

$$\mathcal{B}_{\mathcal{EPR}\mathcal{A},\text{distinct}} = \{ {}_m \circledast a_i^j \mid 0 \leq a \leq 4m - 1 \wedge 0 < i, j < 2m \}$$

where i and j are the distance sectors as defined in Eqs. 2 and Eq. 4 (or alternative distance sector names) and a is the number of the cardinal direction sector of B which contains A as described in Section 3.2 (or, alternatively, the abbreviated cardinal direction name for $m = 2$).

The set $\mathcal{B}_{\mathcal{EPR}\mathcal{A}}$ of relations clearly is jointly-exhaustive and pairwise-disjoint over the given domain $\mathcal{D}_{\mathcal{EPR}\mathcal{A}}$. The set of general relations for $\mathcal{EPR}\mathcal{A}$, as usual, is considered to be the set of all unions of relations from $\mathcal{B}_{\mathcal{EPR}\mathcal{A}}$. For granularity parameter m , $\mathcal{B}_{\mathcal{EPR}\mathcal{A}}$ has $2m - 1 + (4m) * (2m - 1)^2$ base relations, e.g., 75 for $m = 2$ and 305 for $m = 3$.

4.2 Converse operation

Defining the *converse* operation \sim of an $\mathcal{EPR}\mathcal{A}_m$ base relation is straightforward as both direction and distance components can be treated individually. For non-same cases ($\mathcal{B}_{\mathcal{EPR}\mathcal{A},\text{distinct}}$), the direction component needs to be inflected by adding $4m/2$ modulo the number of sectors, $4m$, while the distance components are exchanged:

$$({}_m \circledast a_i^j)^\sim = {}_m \circledast b_j^i \quad \text{with } b = (2m + a) \bmod 4m \quad (6)$$

For instance, the converse of ${}_2 \circledast 3 \frac{2}{1}$ is ${}_2 \circledast 7 \frac{1}{2}$. For the **same** cases from $\mathcal{B}_{\mathcal{EPR}\mathcal{A},\text{same}}$, the following holds:

$$({}_m \circledast_{\text{same}}^d)^\sim = {}_m \circledast_{\text{same}}^e \quad \text{with } e = 2m - d \quad (7)$$

For instance, the converse of ${}_2 \circledast_{\text{same}}^3$ is ${}_2 \circledast_{\text{same}}^1$. To compute the converse of a general non-base relation, one has to compute the converses of all included base relations and combine the results by taking the union.

4.3 Composition operation

Without a closed formula, we need to compute all entries of the composition table to specify the composition operation for $\mathcal{EPR}\mathcal{A}_2$. We were able to automate the computation of the complete table and by this avoid a time consuming and error-prone manual derivation as has been performed for many other spatial calculi. Our approach is similar to the work reported in [54] in that it is based on real algebraic geometry, i.e., we define a system of equations and inequations over the components of the involved e-points. While [54] uses Gröbner bases, our approach is based on employing cylindrical algebraic decomposition (CAD) [6] as provided by the QEPCAD⁴ solver to determine whether the equational

⁴<http://www.usna.edu/cs/~qepcad/B/QEPCAD.html>

systems for every triple of base relations have a solution and thereby checking their realizability.

For instance, the relation $A \text{ } \underset{2}{\circledast} \underset{se \text{ } \overset{equal}{distant}} B$ can be translated into the following four (in)equations assuming that the coordinates of A and B are (x_A, y_A, δ_A) and (x_B, y_B, δ_B) , respectively:

$$y_A - y_B < 0 \quad \text{and} \quad x_A - x_B > 0 \quad (\text{cardinal direction sector } se) \quad (8)$$

$$\delta_A^2 < (x_A - x_B)^2 + (y_A - y_B)^2 \quad (\text{distance } distant) \quad (9)$$

$$\delta_B^2 = (x_A - x_B)^2 + (y_A - y_B)^2 \quad (\text{distance } equal) \quad (10)$$

For $\mathcal{EPR}\mathcal{A}_2$, non-same relations always result in two quadratic (in)equations for the distance components and a conjunction of two linear (in)equations for the direction component. For same relations, only one distance (in)equation is needed in addition to the two linear equations. For higher granularities, the equation systems get more complicated as angle intervals need to be expressed.

For an arbitrary composition triple of $\mathcal{EPR}\mathcal{A}_2$ base relations (b_1, b_2, b_3) , combining the resulting equations yields an equational system over 9 variables $((x_A, y_A, \delta_A), (x_B, y_B, \delta_B), (x_C, y_C, \delta_C))$ and at most 12 (in)equations. In addition, we have to add the side constraints $\delta_A > 0, \delta_B > 0, \delta_C > 0$. Figure 4.3 shows the resulting overall equational system for the composition $A \text{ } \underset{2}{\circledast} \underset{se \text{ } \overset{equal}{distant}} B \circ B \text{ } \underset{2}{\circledast} \underset{nw \text{ } \overset{close}{equal}} C \stackrel{?}{\supseteq} A \text{ } \underset{2}{\circledast} \underset{distant \text{ } \overset{same}}{C}$ in a format similar to what we use to query QEPCAD in our implementation. We actually use a slightly different order of variables and several optimizations in order to simplify the equational systems and, hence, reduce the computation times.

$$\begin{aligned} \exists x_A, y_A, \delta_A, x_B, y_B, \delta_B, x_C, y_C, \delta_C : \\ & \delta_A > 0 \wedge \delta_B > 0 \wedge \delta_C > 0 \\ & \wedge (y_A - y_B) < 0 \wedge (x_A - x_B) > 0 \\ & \wedge \delta_A^2 < (x_A - x_B)^2 + (y_A - y_B)^2 \\ & \wedge \delta_B^2 = (x_A - x_B)^2 + (y_A - y_B)^2 \\ & \wedge (y_B - y_C) > 0 \wedge (x_B - x_C) < 0 \\ & \wedge \delta_B^2 = (x_B - x_C)^2 + (y_B - y_C)^2 \\ & \wedge \delta_C^2 > (x_B - x_C)^2 + (y_B - y_C)^2 \\ & \wedge (x_A - x_C) = 0 \wedge (y_A - y_C) = 0 \wedge \delta_A < \delta_C \end{aligned}$$

Figure 8: Equational system for $A \text{ } \underset{2}{\circledast} \underset{se \text{ } \overset{equal}{distant}} B \circ B \text{ } \underset{2}{\circledast} \underset{nw \text{ } \overset{close}{equal}} C \stackrel{?}{\supseteq} A \text{ } \underset{2}{\circledast} \underset{distant \text{ } \overset{same}}{C}$.

Checking for existence of a solution for the derived equational systems for each triple with QEPCAD required between 0 and 152 seconds on a 2.6 GHz Opteron CPU. We reduced the number of triples that needed to be considered in two ways: (1) The composition table of the cardinal direction calculus [21] was used as an upper approximation: only distance refinements of entries occurring in this table can result in a realizable composition triple. (2) Only the entries in which the first relation has a cardinal direction of 4 or 5 or in which the first relation was a same case were computed. The remaining triples were

then derived via symmetry considerations. Overall, 29,187 triples out of 421,875 had to be computed. The resulting composition table was also verified using several tests, including relation algebraic properties that need to be satisfied and random point generation tests similar to the approach described in [24]. This was done to detect potential implementation errors in the software module responsible for setting up the equational systems. The table as well as the complete calculus specification for $\mathcal{EPR}\mathcal{A}_2$ in SparQ⁵ format is available for download on the web [35]. The overall table contains 51,493 valid composition triples, which is about half the size of the table we get over the same set of base relations but only using the cardinal direction information (110,835 triples).

4.4 Algebraic closure and closure under constraints

It is a general observation that while algebraic closure decides consistency for atomic networks over the CDC calculus, going beyond purely absolute direction relations typically has the effect that algebraic closure may not discover all inconsistencies and, hence, the standard backtracking search over atomic networks can also only be used as an approximate consistency checking method. This is, for instance, the case for relative direction calculi such as Flipflop, Dipole, and \mathcal{OPRA}_m for which the problem of deciding consistency over atomic networks has been shown to be NP-hard [56].

We were able to show that, similarly, algebraic closure does not decide consistency of atomic networks over $\mathcal{EPR}\mathcal{A}_2$ relations using the closure under constraints criterion described by Renz and Ligozat [41]. They show that algebraic closure decides consistency over a set of relations \mathcal{R} if and only if no $R \in \mathcal{R}$ can be refined to non-overlapping subatomic relations. Refinement into subatomic relations of a relation $R \in \mathcal{R}$ means that it is possible to give a consistent atomic network in which R holds between objects x, y such that the set of pairs (u, v) that are instantiated to x and y in a solution of the network is a strict subset of R .

The counterexample from Figure 9 shows that it is possible to refine $\mathcal{EPR}\mathcal{A}_2$ relations into two disjunct subatomic relations and, hence, $\mathcal{EPR}\mathcal{A}_2$ is not closed under constraints. The relation that will be split is the relation $D \text{ } \underset{2}{\circledast} \text{ } ne \text{ } \overset{di}{cl} \text{ } A$ which requires D to be somewhere to the northeast of A and outside the circle around A in Figure 9(c) (the distance relation of A with respect to D does not matter here). Using the auxiliary e-point B in relation $B \text{ } \underset{2}{\circledast} \text{ } n \text{ } \overset{eq}{eq} \text{ } A$, the consistent atomic constraint network from Figure 9(a) refines this relation to the colored area *northeast of and close to B* ($D \text{ } \underset{2}{\circledast} \text{ } ne \text{ } \overset{cl}{cl} \text{ } B$). Doing the same with auxiliary e-point C in relation $C \text{ } \underset{2}{\circledast} \text{ } e \text{ } \overset{eq}{eq} \text{ } A$, another refinement can be achieved, this time to the colored region *northeast of and close to C* ($D \text{ } \underset{2}{\circledast} \text{ } ne \text{ } \overset{cl}{cl} \text{ } C$). The consistent atomic network for this refinement is shown in Figure 9(b). Due to the specific distance relationship, it is clear that both refinements are disjunct (see again Figure 9(c)). Hence, $\mathcal{EPR}\mathcal{A}_2$ is not closed under constraints and algebraic closure is not sufficient to decide consistency of atomic networks. Indeed, when combining the two constraint networks from Figures 9(a) and 9(b) using $B \text{ } \underset{2}{\circledast} \text{ } nw \text{ } \overset{di}{di} \text{ } C$, the inconsistency of the resulting network in which D would have to be located in both colored regions simultaneously is not discovered using algebraic closure.

However, our experimental evaluation in the next section will show that, nevertheless, compositional reasoning using algebraic closure for a set of $\mathcal{EPR}\mathcal{A}_2$ statements is useful

⁵<http://www.sfbtr8.uni-bremen.de/project/r3/sparq/> (see also [51, 52])

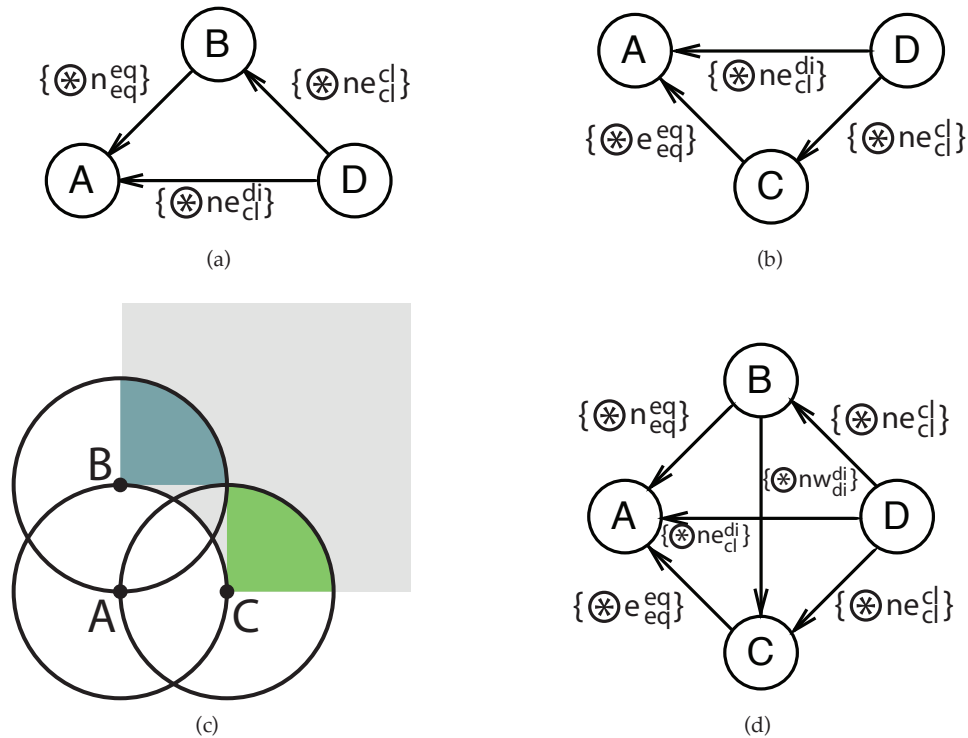


Figure 9: Counterexample that shows that \mathcal{EPRA}_2 is not closed under constraints and, hence, algebraic closure does not decide consistency.

to solve spatial navigation tasks even though it is not sufficient to decide global consistency. This is a similar situation to that for \mathcal{OPRA}_m [36]. In particular, spatial knowledge expressed using \mathcal{EPRA}_2 can be used for deductive reasoning based on constraint propagation, resulting in the generation of useful survey knowledge from local observations. We demonstrate this ability through a direct comparison with the CDC calculus for which algebraic closure is known to decide consistency for a large subset of relations including all base relations [21].

5 Experimental comparison of \mathcal{EPRA}_2 and CDC

The application of qualitative spatial calculi and reasoning techniques for learning the layout of an unknown environment from coarse local observations has been proposed and investigated in [50]. The overall approach is called multi-hypothesis topological mapping (MHTM) because the goal is to derive a graph-based abstraction called *topological map* and the approach tracks multiple distinct graph hypotheses simultaneously. In this work, we are mainly interested in this application as a benchmark to assess and evaluate \mathcal{EPRA}_2 from a computational perspective. The advantage of this benchmark is that it allows us to

investigate properties that are difficult to determine theoretically but nevertheless crucial for application in practice, in particular the trade-off between expressiveness and computational costs in a given qualitative calculus and the effects of only employing incomplete consistency checking techniques such as algebraic closure. We quantify the benefits of the combined direction-distance calculus $\mathcal{EPR}\mathcal{A}_2$ by comparing its performance to that of the CDC calculus without distance information.

In the following, we first give a brief overview on the MHTM framework, describe how we use $\mathcal{EPR}\mathcal{A}_2$ or the cardinal direction calculus to model observations, and then provide experimental results comparing the two calculi.

5.1 The MHTM benchmarking framework

The MHTM approach is best explained by assuming a robot that explores a maze-like environment consisting of hallways and junctions and gathers local observations as shown in Figure 10 (left). The observation history $H = \langle J_1, H_1, J_2, H_2, \dots, H_{n-1}, J_n \rangle$ for a particular exploration run consists of a sequence of alternating junction observations J_i and hallway observations H_j . We assume that the local observations are given in terms of coarse but reliably perceivable categories, namely the relations from a qualitative calculus. For instance, junction observations can be given in terms of cardinal direction relations of the leaving hallways, e.g., hallway h_1 *sw* J_1 and hallway h_2 *s* J_1 for junction observation J_1 in Figure 10. Hallway observations simply are assumed to contain the information which hallway was chosen when leaving a junction. This information is represented by the relative offsets between the chosen hallway and the hallway via which the robot arrived at the junction in the cyclic order of hallways observed. The mapping problem now is to determine the smallest graph structure that would form a valid explanation of the qualitative observations where size is measured in terms of the number of nodes in the graph. A particular graph hypothesis, for instance the one in Figure 10 (right), is valid if it can be drawn into the plane such that all the spatial constraints between the junctions and hallways as implied by the qualitative relations in the local observations are satisfied.

The MHTM approach to the topological mapping problem is to track possible graph hypotheses about the layout of the environment in a tree structure as illustrated in Figure 11. The successors of a node in the tree are constructed by incorporating the next observation. Incorporating a new observation involves two things: (1) changes to the graph structure such as introducing new connections and (2) a check whether the set of implied spatial constraints is consistent, meaning that the hypothesis is valid. For this check, qualitative spatial reasoning techniques for checking consistency are employed such as the path consistency or algebraic closure algorithm [25, 28, 48]. When a hypothesis is found to be inconsistent, it is discarded and the corresponding branch in the tree is closed. Moreover, a search strategy can be used to determine the smallest hypothesis without necessarily considering all valid hypotheses in the tree. An A* search based on admissible estimates of the final solution size, for instance, usually allows for ignoring large parts of the search space (for details, we refer to [49, 50]).

When comparing different qualitative calculi in this benchmarking framework, we use random graph environments and random walks through these graphs, and formulate the observations in terms of relations from these calculi. We then perform the search and record relevant performance parameters to measure the solution quality and the size of the traversed search space. In general, the more expressive a qualitative calculus is, the smaller

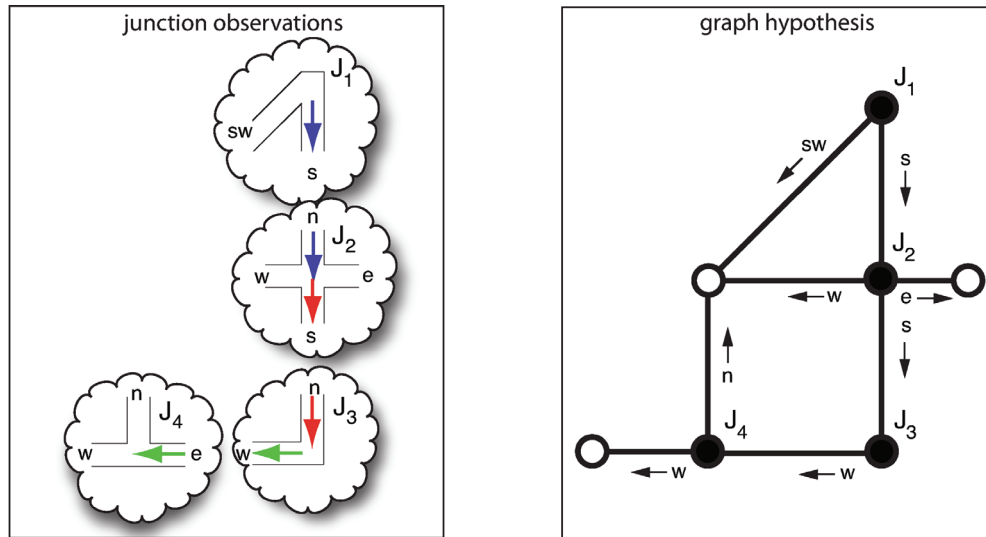


Figure 10: A robot explores a maze-like environment and gathers local observations. A map hypothesis represents the potential layout of the environment. It is valid if the resulting network of constraints implied by the observed spatial relations is consistent.

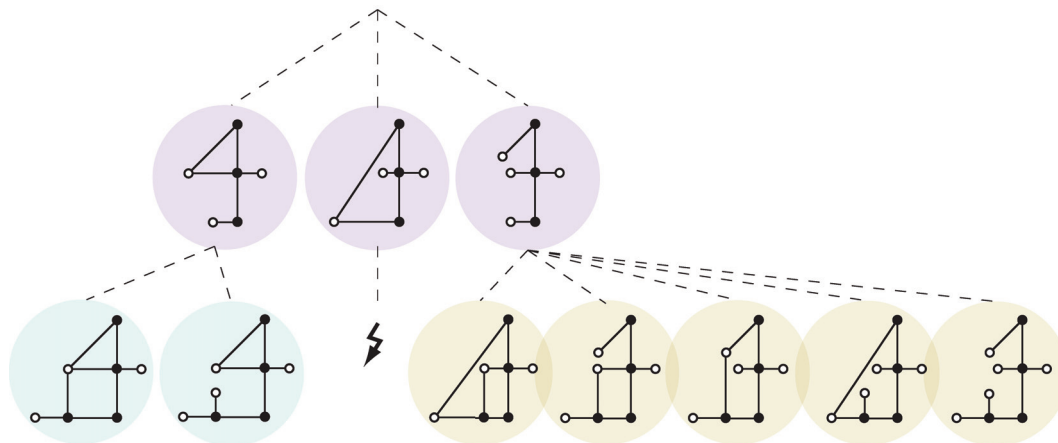


Figure 11: Search tree of graph hypotheses in the MHTM benchmarking approach for the example from Figure 10 (example adopted from [50]).

the ambiguity in the available information which should in principle lead to a better solution quality and a smaller number of node expansions. However, high expressiveness usually also leads to a high computational complexity of the consistency decision procedure overall and the fact that procedures such algebraic closure become incomplete so that not all inconsistencies may be discovered. This can counter the aforementioned benefits

such that these aspects have to be evaluated in combination in order to get a clear picture of how different calculi compare to each other. A merit of the MHTM framework is that it allows for performing this combined analysis.

5.2 Modeling observations with CDC and $\mathcal{E}PRA_m$

Figure 12 shows how a graph hypothesis is converted into a CDC constraint network as already described in [50]. A variable is introduced for each node / junction in the hypothesis, and cardinal direction relations from the junction observations are turned into constraints between the respective variables in the QCN, e.g., $A \text{ ne } B$. The constraints between all non-neighbored junctions are set to $U \setminus \{same\}$ (not shown in the constraint network in the figure).

Using $\mathcal{E}PRA_m$ relations for representing junction and hallway observations allows us to not only model the absolute direction between two junctions but also the relative lengths of two corridors leaving from the same junction. A QCN is derived by introducing an e-point for each pair of node and adjacent edge (or junction and adjacent hallway), as depicted in Figure 13. The variable names are derived by combing the name of the junction with that of the junction to which the respective hallway leads (e.g., AB for the e-point representing junction A and the hallway leading from A to B). For the two variables that represent the different ends of the same hallway (e.g., AB and BA), a constraint is introduced whose direction component is that contained in the junction observations, analogously to the way it is done in the CDC modeling. The distance components are both *equal* as they represent the length of the same corridor (e.g., $AB \text{ }_2\text{ } \otimes \text{ ne } \overset{equal}{\text{equal}} \text{ } BA$). For variables introduced for the same junction but different hallways, for instance BA and BC , the introduced constraint is a *same* relation derived from the perceived relative lengths of the two involved corridors, e.g., $BA \text{ }_2\text{ } \otimes \overset{close}{\text{same}} \text{ } BC$ in the example where the hallway connecting B and A is longer than the one connecting B and C . All other constraints are set to $U \setminus \{ \text{ }_2\text{ } \otimes \overset{close}{\text{same}}, \text{ }_2\text{ } \otimes \overset{equal}{\text{same}}, \text{ }_2\text{ } \otimes \overset{distant}{\text{same}} \}$ to prevent co-location of junctions that are distinct in the hypothesis.

Overall, the number of variables in the derived QCN for a graph hypothesis with m nodes and n edges is m in the case of CDC, while it is $2 \times n$ for $\mathcal{E}PRA_m$. Ignoring those constraints which are the universal relation minus the respective *same* cases, the number of introduced constraints is n for CDC and in $O(n + m k^2)$ for $\mathcal{E}PRA_m$ where k is the highest node degree occurring in the hypothesis.

5.3 Experiments and results

Our evaluation for the most part follows the approach taken in [50] but using $\mathcal{E}PRA_2$ and CDC instead of $\mathcal{O}PRA_2$. While in [50] two variants of the MHTM approach are considered, we only employ the more challenging variant referred to as CompEnv, in which the hypotheses contain assumptions about unvisited junctions and how non-traversed hallways may be connected. Randomly generated graph environments of varying size are generated together with random walks through the graphs in order to generate instances of observation histories which are then fed into the MHTM system. An example environment and walk is shown in Figure 14.

As both the size of the environment as well as the length of the walk affect the difficulty of the problem instance, we use the number of junctions of the correct hypothesis



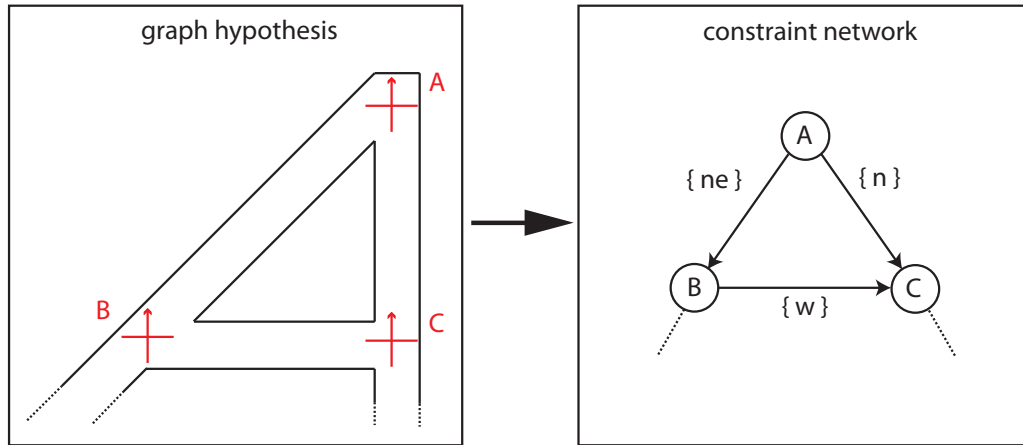


Figure 12: Constraint network extraction for a given graph hypothesis for CDC.

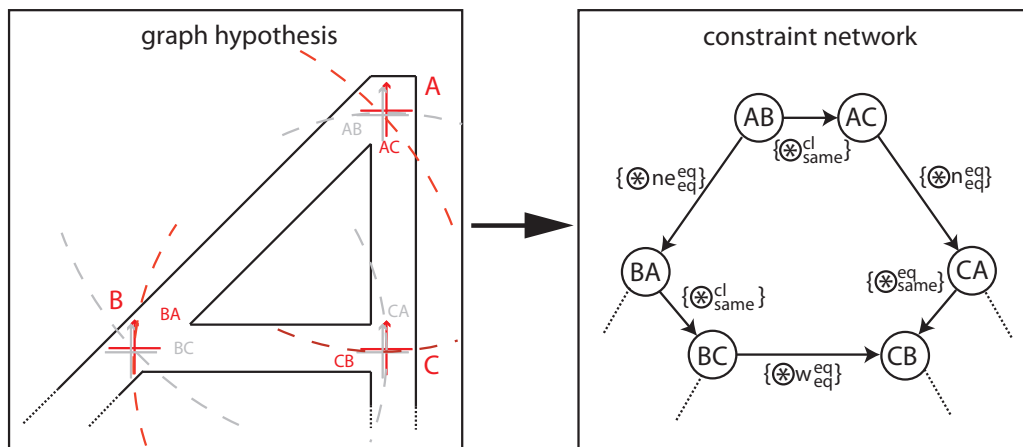


Figure 13: Constraint network extraction for a given graph hypothesis for \mathcal{EPR}_{A_2} .

to measure the *size* of the problem instances and record different performance criteria in dependency of this parameter. The recorded criteria are meant to capture the effect of the chosen calculus in combination with algebraic closure for consistency checking on (1) the solution quality and number of valid models and (2) the traversed search space and number of hypotheses that have to be tracked simultaneously.

The *solution quality* of the final hypothesis h that is computed by the MHTM algorithm is measured by an error measure $e(h)$ which simply sums up how often two junction observations that correspond to different junctions have been mapped to the same node in h and how often two observations corresponding to the same junction have not been mapped to the same node. Moreover, we compute the number of *valid models* up to the same size as the correct model as an assessment of the degree of ambiguity in a given calculus. To de-

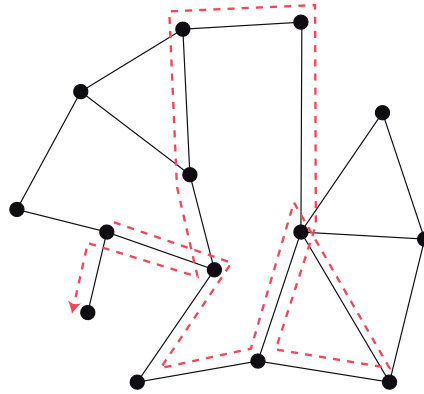


Figure 14: Example of the random problem instances used in the experiments.

termine the number of valid models, a modified version of the MHTM is employed using a complete traversal of the search tree up to the size of correct hypothesis instead of the heuristically guided A* search.

Regarding the search space, we record (a) the number of *expansion steps* in which successors of a hypothesis in the search tree are generated and (b) the *maximal queue size* occurring during the search. The first gives an indication of the time complexity of the approach, while the second is a measure for the space-consumption as it shows how many hypotheses had to be tracked simultaneously. To examine the search space criteria independently the effects of the given calculus on the solution quality, we again use the mentioned modified MHTM approach that traverses the search space up to the depth on which the correct hypotheses can be found. Otherwise, a calculus with worse average solution quality might appear better than it is because the search on average stops already on a higher level in the search tree.

In the following, we summarize the results with respect to solution quality and search space.

5.3.1 Solution quality

We performed 272 runs of the random environment / random walk experiment increasing the size of the problem instances from $size = 4$ to 20 (meaning the correct solution had $size$ nodes). The length of the random walks which determines the length of the observation history was randomly varied between $0.5 \times size$ and $2 \times size$. The resulting error distances averaged over all runs are given in Table 1, while Figure 15 shows the development for increasing $size$ values. We see that the higher expressiveness resulting from the additional distance information leads to a noticeable reduction in the average error distance and, hence, an improvement of solution quality. Overall the solution quality has improved by 10.5%.

We get the a similar picture when looking at the number of valid models determined in 294 runs using the modified MHTM approach up to a $size = 17$. Figure 16 (left) shows on the left the average number of valid models over the problem size using logarithmic scale for the y-axis because of the exponential growth in the number of models. The fact that the

Calculus	Average solution quality
CDC	2.76
\mathcal{EPR}_{A_2}	2.47

Table 1: Solution quality averaged over all runs.

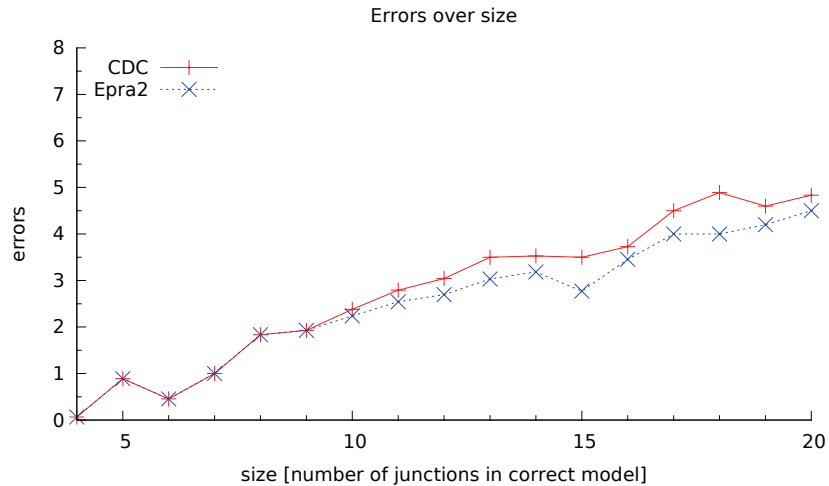


Figure 15: Solution quality (measured in terms of error distance) over problem size.

additional distance information leads to a rather significant reduction is more clearly illustrated in the graph from Figure 16 (right) which directly depicts the reduction percentage over the problem size, reaching 30.0% for $size = 17$. Table 2 contains the model numbers averaged over all runs showing a 25.3% reduction overall.

Calculus	Average number of valid models
CDC	385.557
\mathcal{EPR}_{A_2}	288.158

Table 2: Number of valid models averaged over all runs.

5.3.2 Search space

The search space criteria were computed during the same set of runs used for the valid model numbers. Table 3 summarizes the results regarding the number of node expansion steps performed and the maximal queue size occurring during the search averaged over all runs. It shows an 18.16% reduction in the number of node expansions and a 17.64% reduction in the maximal queue size.

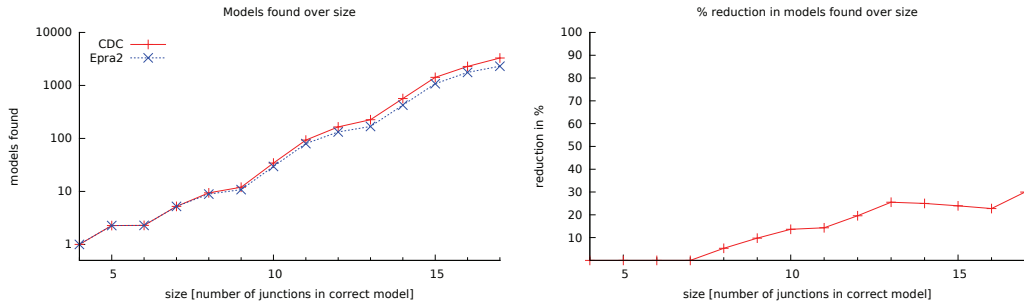


Figure 16: Left: Number of valid models over increasing problem size using logarithmic scale. Right: Reduction in possible models achieved by $\mathcal{E}PRA_2$ compared to CDC.

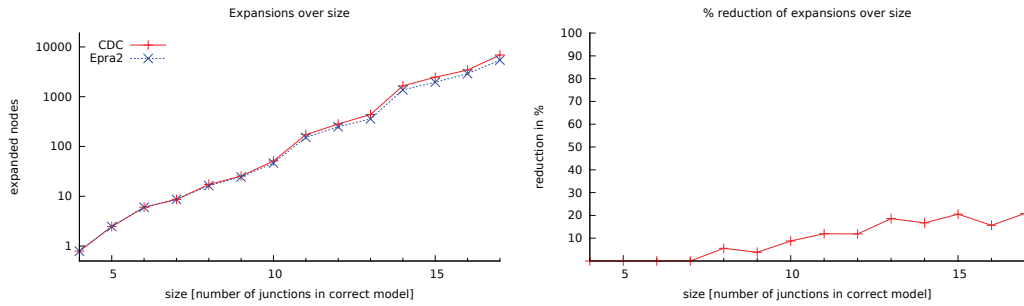


Figure 17: Left: Number of node expansion steps over increasing problem size using logarithmic scale. Right: Reduction in expansion steps achieved by $\mathcal{E}PRA_2$ compared to CDC.

A more detailed view showing the development of the expansions steps required over the problem size is given in Figure 17 (left). Due to the exponential growth, a logarithmic scale is again used for the y-axis. The right graph in Figure 17 therefore directly shows the reduction in expansion steps over the problem size, reaching 20.9% for $size = 17$.

Calculus	Average number of expansions	Average maximal queue size
CDC	732.40	388.97
$\mathcal{E}PRA_2$	599.43	320.34

Table 3: Average number of expansion steps and average maximal queue size as a measure of search space pruning efficiency.

Figure 18 illustrates the increase in the maximal queue size for larger problem instances. For $size = 17$, the average maximal queue size reaches 3078.2 for $\mathcal{E}PRA_2$ and 3944.9 for CDC, a 22.0% reduction achieved by $\mathcal{E}PRA_2$.

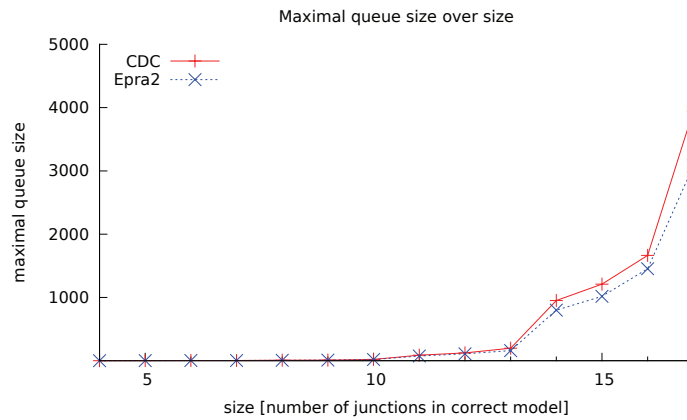


Figure 18: Average maximal queue size over increasing problem size.

5.3.3 Discussion

As described in Section 5.2, the constraint networks generated for $\mathcal{E}PRA_2$ are significantly larger than the corresponding networks for CDC. As a consequence, spatial information in the form of constraints needs to be propagated over more steps which may result in inconsistencies remaining undiscovered over longer time spans in the search when using algebraic closure for consistency checking. Our results show overall improvements in the range of 10% to 26% over the different criteria. These values clearly show that the increased expressiveness of $\mathcal{E}PRA_2$ stemming from the additional distance information is not negated by a decreased effectiveness of algebraic closure. While the improvements can be seen as being rather moderate, $\mathcal{E}PRA_2$ in combination with algebraic closure is an effective formalism for reasoning about positional information, albeit coming at the price of an significant increase in the number of base relations compared to purely directional calculi such as CDC.

6 Conclusions and future work

Not many qualitative spatial calculi exist that support full positional reasoning including both direction and distance information and, to our knowledge, none that in addition have an adjustable granularity such that their resolution can be adapted to the task at hand. In this article, we generalized the idea of attaching hidden reference features to point entities, already used in \mathcal{OPRA}_m , and employed it to develop $\mathcal{E}PRA_m$, a multi-granular positional extension of the CDC that combines absolute direction information with distance information by attaching an internal reference distance to points in the plane. The composition table for $\mathcal{E}PRA_2$ has been determined using an real algebraic geometry approach. The complete specification of $\mathcal{E}PRA_2$ is available as a calculus specification for the SparQ toolbox [35].

We showed that algebraic closure is not sufficient for deciding consistency of atomic $\mathcal{E}PRA_2$ networks. To investigate the performance of $\mathcal{E}PRA_2$ in comparison to CDC, in

particular the trade-off between expressiveness and effectiveness of algebraic closure for consistency checking, we applied the calculus in a benchmark scenario in which graph layouts of unfamiliar environments have to be derived from local observations. The evaluation showed improvements in the range of 10% to 26% for different performance criteria regarding both the quality of the solution and the size of search space that needs to be traversed. The fact that \mathcal{EPRA}_2 in combination with algebraic closure performs better than CDC in these experiments demonstrates that the calculus makes effective use of the additional distance information and that this effect is not negated by a reduction of the effectiveness of algebraic closure to detect inconsistencies.

We will pursue the derivation of complete specifications for higher granularity parameters as part of future research. Moreover, we will aim at investigating and deriving similar specifications for the extended version of \mathcal{OPRA}_m , tentatively called \mathcal{EOPRA}_m , and compare its performance with the original version as well as \mathcal{EPRA}_m using the MHTM benchmarking approach. Also we will investigate how to model extended spatial objects efficiently using elevated points and augmented points in general. For example one can represent objects with their bounding boxes and then model the corners with elevated points. The local reference distances would then correspond to distances between corners of the bounding box. Another aspect for future work is the investigation of spatio-temporal reasoning with direction and distance information based on the notion of conceptual neighborhood for which suitable neighborhood structures over the relations of \mathcal{EPRA}_m (or the other proposed extended calculi) need to be derived.

Acknowledgments

The authors would like to thank André Scholz and Frank Dylla for interesting and helpful discussions related to the topic of the paper and the anonymous reviewers for their valuable comments and suggestions. The work was supported by the National Science Foundation under Grant No. CDI-1028895.

References

- [1] BERENDT, B. Modelling subjective distances. In *Proc. 21st Annual German Conference on Artificial Intelligence (KI-97)*, G. Brewka, C. Habel, and B. Nebel, Eds., vol. 1303 of *Lecture Notes in Computer Science*. Springer, Berlin, 1997, pp. 195–206. doi:10.1007/3540634932_15.
- [2] BILLEN, R., AND CLEMENTINI, E. A model for ternary projective relations between regions. In *Advances in Database Technology, Proc. 9th International Conference on Extending Database Technology (EDBT) (2004)*, E. Bertino, S. Christodoulakis, D. Plexousakis, V. Christophides, M. Koubarakis, K. Böhm, and E. Ferrari, Eds., vol. 2992 of *Lecture Notes in Computer Science*, pp. 310–328. doi:10.1007/978-3-540-24741-8_19.
- [3] CLEMENTINI, E., FELICE, P. D., AND HERNANDEZ, D. Qualitative representation of positional information. *Artificial Intelligence* 95 (1997), 317–356. doi:10.1016/S0004-3702(97)00046-5.

- [4] COHN, A. G., AND HAZARIKA, S. M. Qualitative spatial representation and reasoning: An overview. *Fundamenta Informaticae* 46, 1–2 (2001), 1–29.
- [5] COHN, A. G., AND RENZ, J. Qualitative spatial reasoning. In *Handbook of Knowledge Representation*, F. van Harmelen, V. Lifschitz, and B. Porter, Eds. Elsevier, 2007.
- [6] COLLINS, G. E. Quantifier elimination by cylindrical algebraic decomposition—twenty years of progress. In *Quantifier Elimination and Cylindrical Algebraic Decomposition*, B. F. Caviness and J. R. Johnson, Eds. Springer, Berlin, 1998, pp. 8–23.
- [7] CONDOTTA, J.-F., LIGOZAT, G., AND SAADE, M. A generic toolkit for n-ary qualitative temporal and spatial calculi. In *Proc. 13th International Symposium on Temporal Representation and Reasoning (TIME)* (Budapest, Hungary, 2006). doi:10.1109/TIME.2006.2
- [8] DYLLA, F., FROMMBERGER, L., WALLGRÜN, J. O., WOLTER, D., WÖLFL, S., AND NEBEL, B. SailAway: Formalizing navigation rules. In *Proc. Artificial and Ambient Intelligence Symposium on Spatial Reasoning and Communication (AISB)* (2007).
- [9] EGENHOFER, M., AND FRANZOSA, R. Point-set topological spatial relations. *International Journal of Geographical Information Systems* 5, 2 (1991), 161–174. doi:10.1080/02693799108927841.
- [10] FRANK, A. U. Qualitative spatial reasoning: Cardinal directions as an example. *International Journal of Geographical Information Science* 10, 3 (1996), 269–290. doi:10.1080/02693799608902079.
- [11] FREKSA, C. Using orientation information for qualitative spatial reasoning. In *Theories and Methods of Spatio-temporal Reasoning in Geographic Space*, A. U. Frank, I. Campari, and U. Formentini, Eds., vol. 639 of *Lecture Notes in Computer Science*. Springer, 1992, pp. 162–178. doi:10.1007/3-540-55966-3.10.
- [12] FREKSA, C. Spatial cognition: An AI perspective. In *Proc. 16th European Conference on Artificial Intelligence (ECAI)* (Amsterdam, 2004), R. L. de Mántaras and L. Saitta, Eds., IOS Press, pp. 1122–1128.
- [13] FREKSA, C., MORATZ, R., AND BARKOWSKY, T. Schematic maps for robot navigation. In *Spatial Cognition II*, vol. 1849 of *Lecture Notes in Computer Science*. Springer, Berlin, 2000, pp. 100–114. doi:10.1007/3-540-45460-8.8.
- [14] GALTON, A. *Qualitative Spatial Change*. Oxford University Press, Oxford, UK, 2000.
- [15] GIBSON, J. *The Ecological Approach to Visual Perception*. Houghton Mifflin, Boston, MA, 1979.
- [16] GOYAL, R., AND EGENHOFER, M. Consistent queries over cardinal directions across different levels of detail. *Proc. 11th International Workshop on Database and Expert System Applications* (2000), 876–880. doi:10.1109/DEXA.2000.875129.
- [17] ISLI, A., AND COHN, A. G. A new approach to cyclic ordering of 2D orientations using ternary relation algebras. *Artificial Intelligence* 122, 1–2 (2000), 137–187. doi:10.1016/S0004-3702(00)00044-8.

- [18] LADKIN, P., AND MADDUX, R. On binary constraint problems. *Journal of the ACM* 41, 3 (1994), 435–469. doi:10.1145/176584.176585.
- [19] LADKIN, P., AND REINEFELD, A. Effective solution of qualitative constraint problems. *Artificial Intelligence* 57 (1992), 105–124. doi:10.1016/0004-3702(92)90106-8.
- [20] LIGOZAT, G. Qualitative triangulation for spatial reasoning. In *Spatial Information Theory: A Theoretical Basis for GIS (COSIT'93)*, A. U. Frank and I. Campari, Eds., vol. 716 of *Lecture Notes in Computer Science*. Springer, Berlin, 1993, pp. 54–68.
- [21] LIGOZAT, G. Reasoning about cardinal directions. *Journal of Visual Languages and Computing* 9, 1 (1998), 23–44.
- [22] LIGOZAT, G. Categorical methods in qualitative reasoning: The case for weak representations. In *Spatial Information Theory*, A. Cohn and D. Mark, Eds., vol. 3693 of *Lecture Notes in Computer Science*. Springer, Berlin, 2005, pp. 265–282. doi:10.1007/11556114_17.
- [23] LIGOZAT, G., AND RENZ, J. What is a qualitative calculus? A general framework. In *Proc. of PRICAI-04 (2004)*, C. Zhang, H. W. Guesgen, and W.-K. Yeap, Eds., pp. 53–64. doi:10.1007/978-3-540-28633-2_8.
- [24] LIU, W., AND LI, S. On a semi-automatic method for generating composition tables. In *Proc. IJCAI-2011 Workshop on Benchmarks and Applications of Spatial Reasoning (2011)*, pp. 53–58.
- [25] MACKWORTH, A. Consistency in networks of relations. *Artificial Intelligence* 8, 1 (1977), 99–118. doi:10.1016/0004-3702(77)90007-8.
- [26] MADDUX, R. Some varieties containing relation algebras. *Transactions of the AMS* 272, 2 (1982), 501–526.
- [27] MIENE, A., VISSER, U., AND HERZOG, O. Recognition and prediction of motion situations based on a qualitative motion description. In *RoboCup 2003: Robot Soccer World Cup VII*, D. Polani, B. Browning, A. Bonarini, and K. Yoshida, Eds., vol. 3020 of *Lecture Notes in Computer Science*. Springer, Berlin, 2004, pp. 77–88. doi:10.1007/978-3-540-25940-4_7.
- [28] MONTANARI, U. Networks of constraints: Fundamental properties and applications to picture processing. *Information Science* 7, 2 (1974), 95–132.
- [29] MORATZ, R. Representing relative direction as a binary relation of oriented points. In *Proc. European Conference on Artificial Intelligence (ECAI) (2006)*, G. Brewka, S. Coradeschi, A. Perini, and P. Traverso, Eds., vol. 141 of *Frontiers in Artificial Intelligence and Applications*, IOS Press, pp. 407–411.
- [30] MORATZ, R., LÜCKE, D., AND MOSSAKOWSKI, T. A condensed semantics for qualitative spatial reasoning about oriented straight line segments. *Artificial Intelligence* 175, 16–17 (2011), 2099–2127. doi:10.1016/j.artint.2011.07.004.

- [31] MORATZ, R., NEBEL, B., AND FREKSA, C. Qualitative spatial reasoning about relative position: The tradeoff between strong formal properties and successful reasoning about route graphs. In *Spatial Cognition III*, C. Freksa, W. Brauer, C. Habel, and K. Wender, Eds., vol. 2685 of *Lecture Notes in Artificial Intelligence*. Springer, Berlin, 2003, pp. 385–400.
- [32] MORATZ, R., RENZ, J., AND WOLTER, D. Qualitative spatial reasoning about line segments. In *Proc. European Conference on Artificial Intelligence (ECAI) (2000)*, pp. 234–238.
- [33] MORATZ, R., AND WALLGRÜN, J. O. Propagation of distance and orientation intervals. In *Proc. IEEE/RSJ International Conference on Intelligent Robots and Systems (IROS) (2003)*, pp. 3245–3250. doi:10.1109/IROS.2003.1249656.
- [34] MORATZ, R., AND WALLGRÜN, J. O. Spatial reasoning about relative orientation and distance for robot exploration. In *Spatial Information Theory: Foundations of Geographic Information Science*, W. Kuhn, M. Worboys, and S. Timpf, Eds., *Lecture Notes in Computer Science*. Springer, Berlin, 2003, pp. 61–74.
- [35] MORATZ, R., AND WALLGRÜN, J. O. EPRA2 specification for SparQ, 2012. doi:10.5311/JOSIS.2011.5.84.epra-2-2.lisp.
- [36] MOSSAKOWSKI, T., AND MORATZ, R. Qualitative reasoning about relative direction of oriented points. *Artificial Intelligence 180–181* (2012), 34–45. doi:10.1016/j.artint.2011.10.003.
- [37] NEBEL, B., AND BÜRCKERT, H.-J. Reasoning about temporal relations: A maximal tractable subclass of allen’s interval algebra. *Journal of the ACM* 42, 1 (1995), 43–66. doi:10.1145/200836.200848.
- [38] NEBEL, B., AND FREKSA, C. Ai approaches to cognitive systems—The example of spatial cognition. *Informatik Spektrum* 34, 5 (2011), 462–468. doi:10.1007/s00287-011-0555-6.
- [39] POMMERENING, F., WÖLFL, S., AND WESTPHAL, M. Right-of-way rules as use case for integrating golog and qualitative reasoning. In *KI (Berlin, 2009)*, B. Mertsching, M. Hund, and M. Z. Aziz, Eds., vol. 5803 of *Lecture Notes in Computer Science*, Springer, pp. 468–475. doi:10.1007/978-3-642-04617-9_59.
- [40] RANDELL, D. A., CUI, Z., AND COHN, A. G. A spatial logic based on regions and connection. In *Proc. Conference on Principles of Knowledge Representation (KR)*, B. Nebel, C. Rich, and W. Swartout, Eds. Morgan Kaufmann, 1992, pp. 165–176.
- [41] RENZ, J., AND LIGOZAT, G. Weak composition for qualitative spatial and temporal reasoning. In *Principles and Practice of Constraint Programming - CP 2005, 11th International Conference, Proceedings*, P. van Beek, Ed., vol. 3709 of *Lecture Notes in Computer Science*. Springer, Berlin, 2005, pp. 534–548. doi:10.1007/11564751_40.
- [42] RENZ, J., AND MITRA, D. Qualitative direction calculi with arbitrary granularity. In *Proc. of PRICAI-04*, C. Zhang, H. W. Guesgen, and W.-K. Yeap, Eds., vol. 3157 of *Lecture Notes in Computer Science*. Springer, Berlin, 2004, pp. 65–74. doi:10.1007/978-3-540-28633-2_9.

- [43] RENZ, J., AND NEBEL, B. On the complexity of qualitative spatial reasoning: A maximal tractable fragment of the region connection calculus. *Artificial Intelligence* 108, 1–2 (1999), 69–123. doi:10.1016/S0004-3702(99)00002-8.
- [44] RENZ, J., AND NEBEL, B. Qualitative spatial reasoning using constraint calculi. In *Handbook of Spatial Logics*, M. Aiello, I. E. Pratt-Hartmann, and J. F. van Benthem, Eds. Springer, Berlin, 2007, pp. 161–215. doi:10.1007/978-1-4020-5587-4_4.
- [45] SCHLIEDER, C. Reasoning about ordering. In *Spatial Information Theory: A theoretical basis for GIS*, A. Frank and W. Kuhn, Eds., vol. 988 of *Lecture Notes in Computer Science*. Springer, Berlin, 1995, pp. 341–349.
- [46] SCIVOS, A., AND NEBEL, B. The finest of its class: The practical natural point-based ternary calculus LR for qualitative spatial reasoning. In *Spatial Cognition IV*, C. Freksa, M. Knauff, B. Krieg-Brückner, B. Nebel, and T. Barkowsky, Eds., *Lecture Notes in Artificial Intelligence*. Springer, Berlin, 2005, pp. 283–303.
- [47] TARSKI, A. On the calculus of relations. *Journal of Symbolic Logic* 6 (1941), 73–89.
- [48] VAN BEEK, P. Reasoning about qualitative temporal information. *Artificial Intelligence* 58 (1992), 297–326.
- [49] WALLGRÜN, J. O. *Hierarchical Voronoi Graphs – Spatial Representation and Reasoning for Mobile Robots*. Springer, Berlin, 2010.
- [50] WALLGRÜN, J. O. Qualitative spatial reasoning for topological map learning. *Spatial Cognition and Computation* 10, 4 (2010), 207–246. doi:10.1080/13875860903540906.
- [51] WALLGRÜN, J. O., FROMMBERGER, L., DYLLA, F., AND WOLTER, D. SparQ User Manual v0.7. User manual, University of Bremen, Jan. 2009.
- [52] WALLGRÜN, J. O., FROMMBERGER, L., WOLTER, D., DYLLA, F., AND FREKSA, C. Qualitative spatial representation and reasoning in the SparQ-toolbox. In *Spatial Cognition V*, T. Barkowsky, M. Knauff, G. Ligozat, and D. Montello, Eds., vol. 4387 of *Lecture Notes in Computer Science*. Springer, Berlin, 2007, pp. 39–58. doi:10.1007/978-3-540-75666-8_3.
- [53] WESTPHAL, M., DORNHEGE, C., WÖLFL, S., GISSLER, M., AND NEBEL, B. Guiding the generation of manipulation plans by qualitative spatial reasoning. *Spatial Cognition and Computation* 11, 1 (2011), 75–102. doi:10.1080/13875868.2010.538952.
- [54] WOLTER, D. Analyzing qualitative spatio-temporal calculi using algebraic geometry. *Spatial Cognition and Computation* 12, 1 (2011), 23–52. doi:10.1080/13875868.2011.586079.
- [55] WOLTER, D., DYLLA, F., WÖLFL, S., WALLGRÜN, J. O., FROMMBERGER, L., NEBEL, B., AND FREKSA, C. SailAway: Spatial cognition in sea navigation. *Künstliche Intelligenz* 1 (2008), 28–30.
- [56] WOLTER, D., AND LEE, J. H. Qualitative reasoning with directional relations. *Artificial Intelligence* 174, 18 (2010), 1498–1507. doi:10.1016/j.artint.2010.09.004.